

Available online at [www.sciencedirect.com](http://www.sciencedirect.com)

SCIENCE @ DIRECT®

Journal of Molecular Graphics and Modelling 23 (2004) 305–315

---

*Journal of  
Molecular  
Graphics and  
Modelling*

---

[www.elsevier.com/locate/JMGM](http://www.elsevier.com/locate/JMGM)

## Ptuba: a tool for the visualization of helix surfaces in proteins

Jaime Arce Lopera\*, James N. Sturgis, Jean-Pierre Duneau

*Laboratoire d'ingénierie des Systèmes Macromoléculaires (UPR 9027), Institut de Biologie Structurale et Microbiologie,  
31 Chemin Joseph Aiguier, 13402 Marseille Cedex 20, France*

Received 23 March 2004; received in revised form 28 September 2004; accepted 15 October 2004

---

### Abstract

Projection of transmembrane helices using a Uniform B-spline Algorithm is a tool for the visualization of interactions between helices in membrane proteins. It allows the user to generate projections of 3D helices, no matter what their deviations from a canonical helix might be. When associated with adapted coloring schemes it facilitates the comprehension of helix-helix interactions. Examples of transmembrane proteins were chosen to illustrate the advantages that this method provides. In the glycoporphin A dimer we can easily appreciate the structural features behind homodimerisation. Using the structure of the fumarate reductase we analyze the contact surfaces inside a helical bundle and thanks to structures from a molecular dynamics simulation we see how modifications in structure and electrostatics relate to their interaction. We propose the use of this tool as an aid to the visualization and analysis of transmembrane helix surfaces and properties.

© 2004 Elsevier Inc. All rights reserved.

*Keywords:* Transmembrane;  $\alpha$  Helix; Projection; Visualization; Helical interactions; Membrane protein

---

### 1. Introduction

Thermodynamic models of  $\alpha$  helical membrane protein assemblies suggest that the folding process can be considered in two distinct stages, insertion of  $\alpha$  helices across the membrane bilayer and subsequent association of transmembrane segments [1,2]. This second step will be driven by surface patterns exposed by each helix that modulate affinity and specificity. For instance, the GxxxG motif is believed to be involved in high affinity associations between two helices [3,4]. Alternatively the modification of specific individual residues involved in electrostatic interactions or hydrogen bonding between helices can modify helix-helix interactions and lead to disease [5].

Furthermore, modifications in the associations between transmembrane segments are often at the center of membrane protein function, one can cite as examples the gating of the mechanosensitive channel MscL [6,7] or Ca transport by the Ca-ATP'ase [8,9] where in each case bending or rotation of helices change the interaction

interfaces and are at the center of functionally important conformation changes. It is therefore crucial to understanding the way these helices interact in order to gain insight not only into the structure of this class of proteins but also into their function.

Visualizing interactions between helices with multiple partners in large membrane proteins or membrane complexes can reveal itself to be a daunting task. Even the visualization of individual helical surfaces is often difficult. Comprehending complex data sets usually leads to the development of more concise representations of their information that renders them more accessible. For instance, the list of  $\Phi$  and  $\psi$  angles in a protein can be far more meaningful in a Ramachandran plot [10–12], structurally important motifs in the sequence of a soluble protein can be more easily visualized using hydrophobic cluster analysis, HCA [13,14] or interfaces between proteins can be more accessible using Molsurfer [15]. To simplify the visualization of the surfaces of 3D helices we describe here a method for producing pseudo 2D projections that can be color coded to represent various aspects of their properties, environment or dynamics. Topological restriction to cylinders makes projection easier than for free form surfaces. However when

---

\* Corresponding author. Tel.: +33 4 91 16 44 85; fax: +33 4 91 71 21 24.  
E-mail address: [arce@ibsm.cnrs-mrs.fr](mailto:arce@ibsm.cnrs-mrs.fr) (J.A.L.).

tracing the axis of these objects it is necessary to keep track of various helical deformations, which are particularly common and indeed important in membrane proteins. Various methods have been used to generate a helix axis, rotational fitting [16], the cross product of triad bisectors [17] or fitting to a helix [18] to name a few. These methods were not really designed with helical deformations in mind and deviations from ideality in the helix often cause problems.

Some of them perform fitting to a line [16], making them unfit to follow the local distortions in real helices. The other methods which use a more local approach but as we will see in a comparison made below, they lack the precision necessary for the rest of the projection or change direction in a undesirable manner in the non ideal regions of the helix. For a more extensive description and comparison of these methods in straight helices see Christopher et al [19].

The idea of projection, transforming a canonical helix into a helical diagram is not a new. Since the discovery of the  $\alpha$  helix [20], understanding helical interactions has brought about new representations [21] of these objects. For instance, the helical wheel where the C $\alpha$  are projected in a plane orthogonal to the axis or the helical net diagram where a helical object is transformed into a series of coordinates on a plane. For a more formal and contemporary description of the latter and how to use these projections, see Walther et al [22]. Nevertheless, this approach has not previously been performed on real structures and no current method (besides the one presented here) is known to achieve this given their characteristic deformations. We are mainly interested in a method similar to the helical net diagram and the helical wheel projection is not currently implemented.

Ptuba is the acronym of Projection of Transmembrane helices using a Uniform B-spline Algorithm. This program, written in python, is freely available under a GPL license from [http://lism.cnrs-mrs.fr/JS\\_files/Ptuba.html](http://lism.cnrs-mrs.fr/JS_files/Ptuba.html). The input for this program consists of two files. The first is the pdb format structure of the protein that contains the helix(es) to be processed. The second file is the annotation file that tells the program what residues from the structure are to be considered. After describing our axis tracing method, we will compare it to other methods in the results section and we will present several examples to illustrate its utility.

## 2. Methods

In Fig. 1, the data flowchart shows how two input files, the annotation file and the pdb file are processed by the program Ptuba. First, the individual helices are extracted from the structure file using the information from the annotation file. Then the atomic coordinates and other information are separated. The atomic coordinates are processed by the two main steps in the algorithm: axis generation and coordinate projection. Finally, the resulting coordinates are duplicated and merged with the non-coordinate information to produce

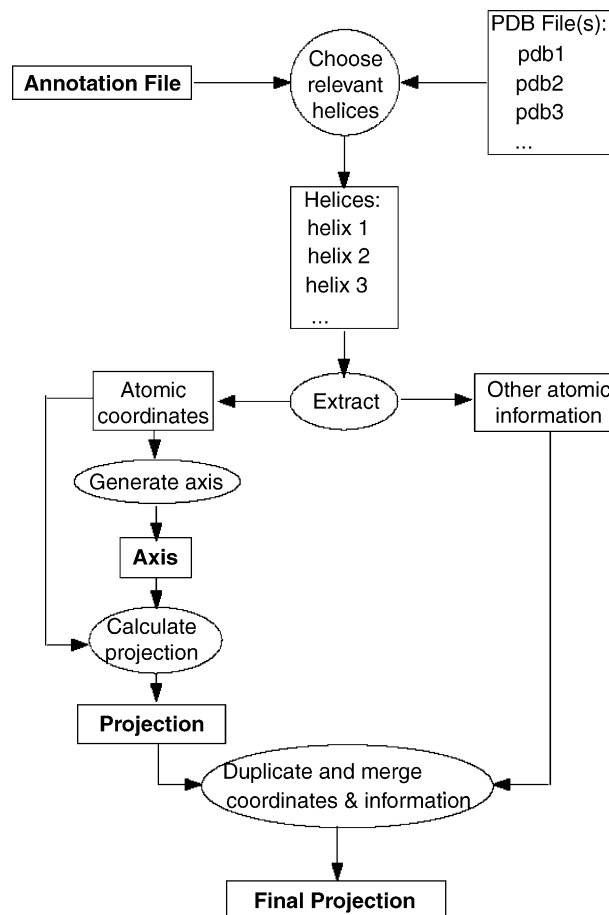


Fig. 1. Program data flow diagram. The input files (annotation, pdb) are processed by parsers so the information concerning the helices of interest are extracted. This information is divided so that the atomic coordinates can be further processed to generate an axis and the projection. Then this information is duplicated as the non-coordinate information and merged to create the final projection that spans more than  $360^\circ$  in order to prevent misrepresentations at the edges.

the final projection. The final projection represents  $360^\circ$  twice ( $720^\circ$ ), as in HCA [13–14] to avoid having an unique feature “broken” in half with part of it near an edge of the projection and the other part on the opposite edge. This way, at least once the feature is complete and can be easily recognized.

The annotation file is constructed in a format inspired by the Mptopo database [23] this choice allows us to use this database. The input protein structure and output projection are both in pdb format in our implementation.

### 2.1. 1. Generating the axis

To generate an axis that can be used for the projection of an  $\alpha$  helical protein segment a number of factors need to be addressed. That axis must be able to accommodate modifications in helicity and the various types of deformations found in proteins. For example, both overwound,  $3^{10}$  turns, underwound  $\pi$  bulges and different kinks with various

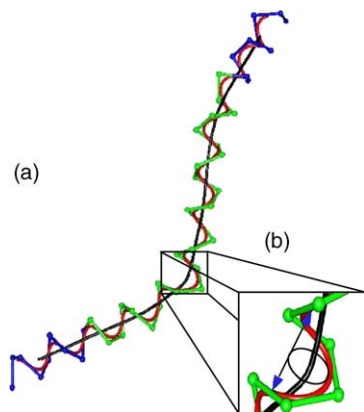


Fig. 2. Generation of the axis. Example of an axis generated by Ptuba. (a) The axis (black) is generated to follow the center of a smooth helical b-spline (red) that in turn is generated using the  $C\alpha$  atoms of the peptide chain as control points. (b) In this inset that enlarges the previous image, the blue arrows represent the vector perpendicular to the plane that will be used to project the portion of the spiral between the two ends of the vector. The result is the brown ellipse.

helix kink and swivel angles [24] are found frequently in membrane protein structures [25]. In addition we need to generate an axis that extends well beyond the last  $C\alpha$  in the segment. It is important that the axis extends far enough for every atom to be projected. For example, a “snorkeling” lysine [26] might find its terminal side-chain atoms to be out of range of the axis. To avoid these problems we add a certain number of  $C\alpha$  (9 by default, which gives an extra 6 Å of axis) to both the C-terminal and N-terminal ends of the helical segment. This is illustrated in Fig. 2, where the helical segments, with  $C\alpha$ 's in green, is extended using canonical parameters for the  $C\alpha$ ' chain (angle  $-89^\circ$ , dihedral  $-40^\circ$ , length 3.8 Å).

## 2.2. Spiral trace: b-spline

Then a uniform b-spline is constructed, shown in red in Fig. 2 that uses this extended set of  $C\alpha$  atoms as control points. A b-spline is fundamentally the result of an interpolation that given a set of points generates of smooth parametric curve that that is influenced a given time by a specific number of these points (order of the b-spline, 5 in our examples) [27]. To generate an axis that faithfully follows the center of this smooth helical curve, and accommodate modifications in the helicity of the segment, we use an algorithm to evaluate the b-spline using a sliding window of variable size to determine what should be considered as a turn of the helix.

## 2.3. Find the best size for a helical turn

To do this in a distorted spiral we project the helical segment in the current window onto the plane perpendicular to the vector between the first and the last point in the window (Fig. 2b). We then compare the projections from

different sized windows and select the projection that most closely resembles a circle. To test for circularity we measure the distance in the projection plane between each projected point on the spline and the center of the set and measure the variance of this distance. The most circular set has a minimal variance. We then calculate the geometrical center of the corresponding spiral slice and use it as a point on the axis.

## 2.4. The axis

The succession of these centers constitutes the axis (Fig. 2a black). This method is able to accommodate all the usual deformations found in transmembrane domains, like bends, kinks, bulges (wider helix turn) and helix tightening, with a reasonable accuracy/time ratio. Using a b-spline allows us to define the axis with a resolution better than the simpler approaches based only on the center of mass of  $C\alpha$  atoms [28]. This accuracy is essential if one wants to preserve in the projection the spatial relationships of the aminoacyl residue located along the faces of the helix, and faithfully represent the various distortions of the axis. We compare this axis to that generated by several other methods below.

## 2.5. II. The projection

Once we have generated an axis, the next step is generation of the projection. This requires the generation of three coordinates for each atom of each amino acid in the segment. These coordinates,  $x'$ ,  $y'$ ,  $z'$ , refer respectively to the depth, lateral advancement, and vertical progression.

## 2.6. Overview

The depth is the distance between the atom and the nearest point on the axis (Fig. 3a,  $x'$  black). Lateral advancement is the position of an atom round the helix, relative to a reference position, this is given by an angle which is multiplied by a fixed radius to calculate the coordinate ( $y'$  red). The vertical progression is calculated as the distances along the helix axis from the start to the point on the axis nearest to the atom ( $z'$  blue).

## 2.7. The reference problem

Lateral advancement is the trickiest coordinate to calculate since in a deformed helix the angle between the vector going from a given atom to its nearest point on the axis and a reference vector will depend not only on the desired torsional angle round the axis but also a contribution derived from deformations in the axis. This contribution is the angle  $\beta$  in Fig. 3b, where, calculating the angle between the two vectors on the same face of the helix, a torsional angle of zero, gives a non-zero result.

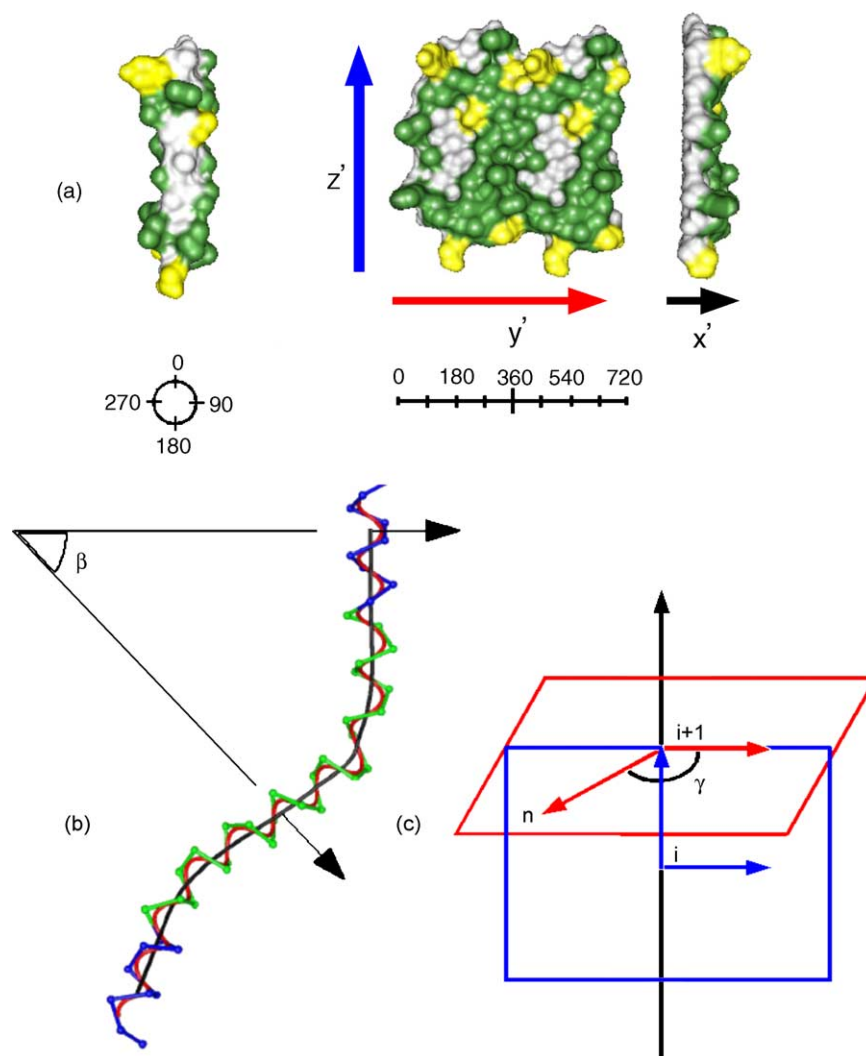


Fig. 3. The projection. Illustration of the projection of transmembrane helix, one of the helices of glycoporphin A (PDB structure 1AFO). (a) The left of the figure shows the surface of the original helix, viewed with chimera, while the right hand part of the figure gives us a frontal and a lateral view of the projected and duplicated surface. On each surface the residues have been colored according to the hydrophobic scheme. The colored arrows represent the different coordinates necessary for the projection  $x'$  (black, distance from the axis),  $y'$  (red, lateral advancement) and  $z'$  (blue, vertical progression). Just below the helix on the left, a small wheel represents schematically the perimeter of the cylinder that represents the helix. To the right, we see the result of the projection of the perimeter and how twice this circle ( $360^\circ$ ) becomes a line ( $720^\circ$ ). (b) This is a projection of the helix in Fig. 2 in 2D where two vectors (arrows in black) form an angle  $\beta$ . The two vectors are part of the same face of the helix. This angle represents a bias when considering lateral advancement only. (c) Here we see how local reference vector at point  $i + 1$  is built at the intersection of two planes and how the unbiased angle  $\gamma$ , used when considering the lateral advancement, is calculated.

## 2.8. The solution

To avoid this difficulty we generate a local reference vector for each point in the axis that takes into account the effects of the deformation. Basically, we will use a face of the helix as reference. As an initial reference we take the vector between the first atom of the helix in the pdb file and the nearest point on the axis. This vector is orthogonal to the axis in that point, as all local reference vectors must be perpendicular to the axis. At point  $i + 1$  on the axis the plane orthogonal to the axis (Fig. 3c red) will contain the local reference vector. The local reference vector at point  $i$  and the vector between the points  $i$  and  $i + 1$  in the axis describe a

second plane (Fig. 3c blue). If the axis distortion between these two points is small enough, the intersection of these two planes gives the local reference vector at point  $i + 1$ . This process is illustrated in Fig. 3c where we can also see the angle  $\gamma$  with atom  $n$ .

To create local reference vectors, we therefore calculate the intersection of these two planes recursively. The resulting local reference vectors allow us to calculate an unbiased angle  $\gamma$  with the corresponding vector between an atom and its nearest point in the axis, thus, obtaining a correct  $y'$  coordinate.

This method of generating the projection is new and is one of the originalities of our program.

### 3. Coloring schemes

As in any map, the coding of the information on the projection is crucial to its intelligibility. We have implemented and use below several color schemes for the projection in order to increase its information content, these schemes color on the basis of atom or residue physico-chemical properties, structure or dynamics. In a first scheme (Hydrophobic) we use physico-chemical properties of the amino acids, a partition of residues into polar/charged (yellow) and hydrophobic (green) classes with white for the main chain. A second scheme (Electrostatics) colors the surface according to their partial charges taken from the amber94 force field [29]. A first simple structure based coloring scheme (Topology) colors the atoms according to their depth coordinate, while a second (Pairwise) color codes the interaction between two transmembrane segments. In this scheme we color atoms according to their distance to the closest atom on the other helix, red for the proximal and blue for distal.

This scheme is inappropriate when dealing with multiple helices. To display structural information in this context we have developed novel coloring scheme (Multiple) that allows us to represent the packing of multiple helices. Here we encode information on the interfaces using the HLS color space. In this scheme the hue encodes the interface between two helices, each interface having a unique hue. Lightness is the amount of black or white in a color. The distance to the other helix affects the lightness, and therefore the atoms closer to the opposing helix are lighter whereas those at a greater distance are darker. Saturation is used to encode the overlapping interfaces e.g.: when residues make simultaneous interactions with several helices. If an atom is found in more than one interface it is the closest helical partner that determines its hue. Since genetic and cultural variation results in individuals understanding colors differently [30–33], we chose to use only pure hues in our scheme instead of mixing colors as this could be confusing. Therefore, in this cases where residues interact with multiple helices we use saturation to code for this making the atoms equally important in different interfaces more gray. We chose to color only the interfacial atoms at less than 5 Å from the interacting helix, the others are colored black.

### 4. Implementation

The projection program has been implemented in Python using the PDB data format for structure input and output. This program uses two kind of files. The first is the pdb format structure(s) of the protein(s) having the helix(es) to be processed. The second file is the annotation file that tells the program what residues from the structure are to be considered as the interesting helix(es). This file may correspond to a single helix or a database containing all the helices to be processed in multiple PDB files.

Python was chosen as the programming language as it is easily transportable it also has the advantage of being very legible and clear but this comes at the price of a reduced computational performance.

Molecular graphics images were produced using the UCSF chimera package from the Computer Graphics laboratory, University of California, San Francisco (supported by NIH P41 RR-01081). The coloring schemes are implemented as extensions of the chimera molecular modeling system [34].

The source code of Ptuba is distributed under the GPL license and is available for download at [http://lism.cnrs-mrs.fr/JS\\_files/Ptuba.html](http://lism.cnrs-mrs.fr/JS_files/Ptuba.html).

### 5. Results and discussion

As mentioned above various other, simpler, methods can be used to generate helix axes and it is important to compare our method with the best of the available methods. As has previously been pointed out [19], there exists no objective standard for the true axis of a helix in a real protein and therefore an objective evaluation of accuracy is not possible. Nevertheless, it is possible to suggest certain desirable properties of the axis, namely smoothness, and passage close to the center of the atoms. In Fig. 4 we compare axes generated by our method (red) with those produced by two other methods P-curve (yellow) [35] and the algorithm used in GAS-P (cyan) [17]. In this figure three deformed helices found in membrane proteins are illustrated.

First, we see clearly that all the methods agree quite well on the path to follow in the straight portions of the helix. However, they differ significantly where deviations from a canonical helix appear. In the deformations (Ptuba) is the one that fits best our intuitive idea of what a helical axis in a distorted helix should be, namely a continuous smooth curve at the center of the pseudo cylindrical hull described by the helix. The other methods lack robustness where they helix deviates from ideality and change direction abruptly many times. An additional advantage of using a spline is that the points described are influenced by a larger number of C $\alpha$  atoms (order of the spline, 5 in our examples) and this allows the smoothing out of local position errors.

To illustrate the utility of the program we present here a series of examples in which we have produced helix projections and show how structural and functional information can be appreciated in these projections.

#### 5.1. Glycophorin A

Fig. 5 shows a set of projections of the two transmembrane helices in Glycophorin A homodimers. This figure allows us to demonstrate some of the ways of coloring the projections. Each of the coloring schemes brings out different pieces of information that helps to obtain a clearer view of the interaction between the two helices. We

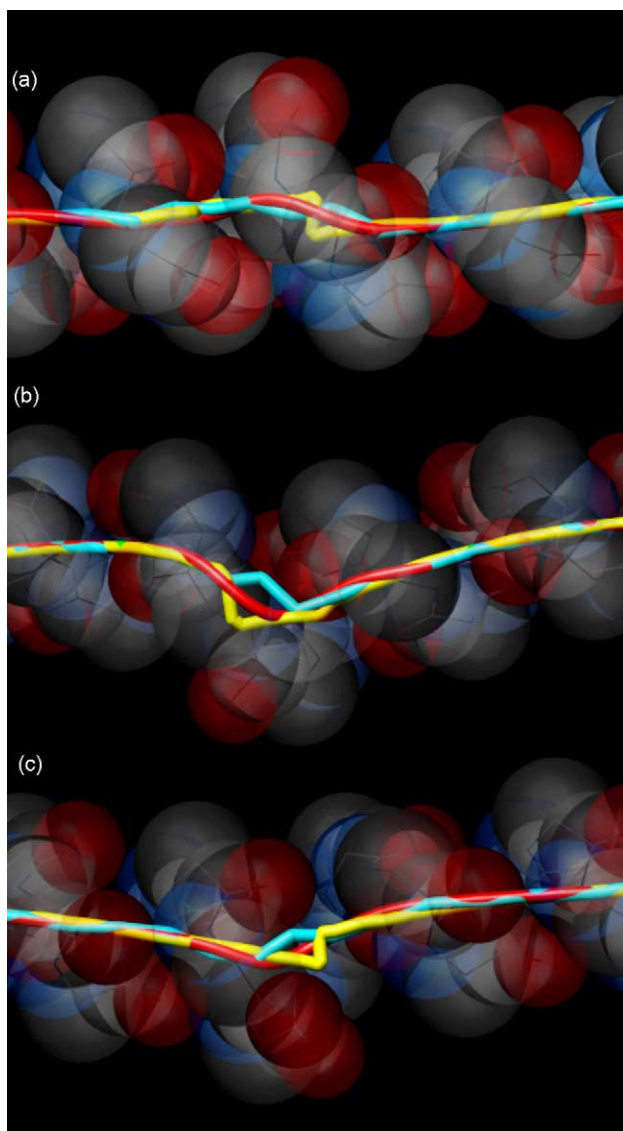


Fig. 4. Comparison of axis tracing methods. Helical deformations are exemplified in this figure by (a) helix 404–433 from chain A of the Cytochrome C Oxidase (1AR1), (b) helix 160–190 from chain A of Halorhodopsin (1E12) and (c) helix 13–35 from chain T of the bovine heart cytochrome C oxidase (1OCR). In each panel we show three axes, the red one generated by Ptuba, the yellow one by pCurves and the blue one using the algorithm used in Gas-P [17].

can see for instance that the two homodimers differ structurally. For example, the tyrosine 93 on the upper left of the projection (Prominent yellow blob in a circle) has its side chain oriented differently. This difference probably arises from the protocol used for the refinement of the model structures and is not necessary meaningful. Nevertheless, the visibility of this difference demonstrates the ability of Ptuba to capture and display subtle structural changes and their repercussion on the surface properties. Using the color code for hydrophobicity (Hydrophobic) we can see clearly the exposure of the helix backbone (in white) due to the presence of Gly residues (Fig. 5a), next to the hydrophobic

side chains colored green and the polar or charged ones yellow.

With a depth color coded representation (Topology) (Fig. 5b) the backbone exposure can be compared with the valley (green–blue) between the brown peaks of the voluminous hydrophobic side chains. Also, this area is richer in charges as we can see using the (Electrostatics) scheme (Fig. 5c). This is in particular due to the C=O in the peptide bond and the nearby OH of Threonine 87. It then comes as no surprise that the dimer interface mostly spans this region as seen in the distance based color code (Pairwise) of the Fig. 5d. The closest atoms are found in Glycine 79 and nearby Valine 80 as seen with this scale where red colors the atoms closest to the other helix and the blue regions are those that are farther apart. In Fig. 5, we are confronted to several images that are telling us quite bluntly that among the defining features of this interaction we can see a surface complementarity induced by this central depression. In comparison the appreciation of this characteristics on a 3D image of the interaction as previously reported [36] are less accessible. It is harder in this kind of representation to fully comprehend the surface complementarity.

## 5.2. Fumarate reductase

To illustrate the possibilities of projections to display the multiple interactions between transmembrane helices in a membrane protein we chose fumarate reductase as an example of a typical  $\alpha$  helical transmembrane bundle with some distorted helices. This protein catalyzes an important step in anaerobic respiration and despite crossing the membrane with two subunits, this bundle is made of only six transmembrane helices (Fig. 6a). This gives us a taste of complexity without having the burden of exploring a bigger bundle. We can also see kinked helices in this bundle (for example helix 4) which is a fairly common phenomenon in transmembrane helical segments. These deformations are responsible for the holes and promontories in the projections of the helix (Fig. 6b). Beyond each particular deformation of the helices, of considerable interest in a helix bundle are the interactions between helices and the various interfaces.

As described above to color the interfaces we used the (Multiple) scheme. The hue that represents each unique interface between two transmembrane helices is shown by the color matrix (Fig. 6 inset). The simplest case of an interface can be found on the upper right corner of Fig. 6b (helix 3). There, two differently colored interfaces imply this helix is in interaction with two other helices. However, this two interfaces constitute a continuous patch with the width of a helix. This indicates this is necessarily an outer helix since otherwise the interfaces would be side by side and no extensive surface would be colored black. We also note that this kind of interaction is a bit unusual since the patches are almost parallel to the helix orientation. Therefore, without

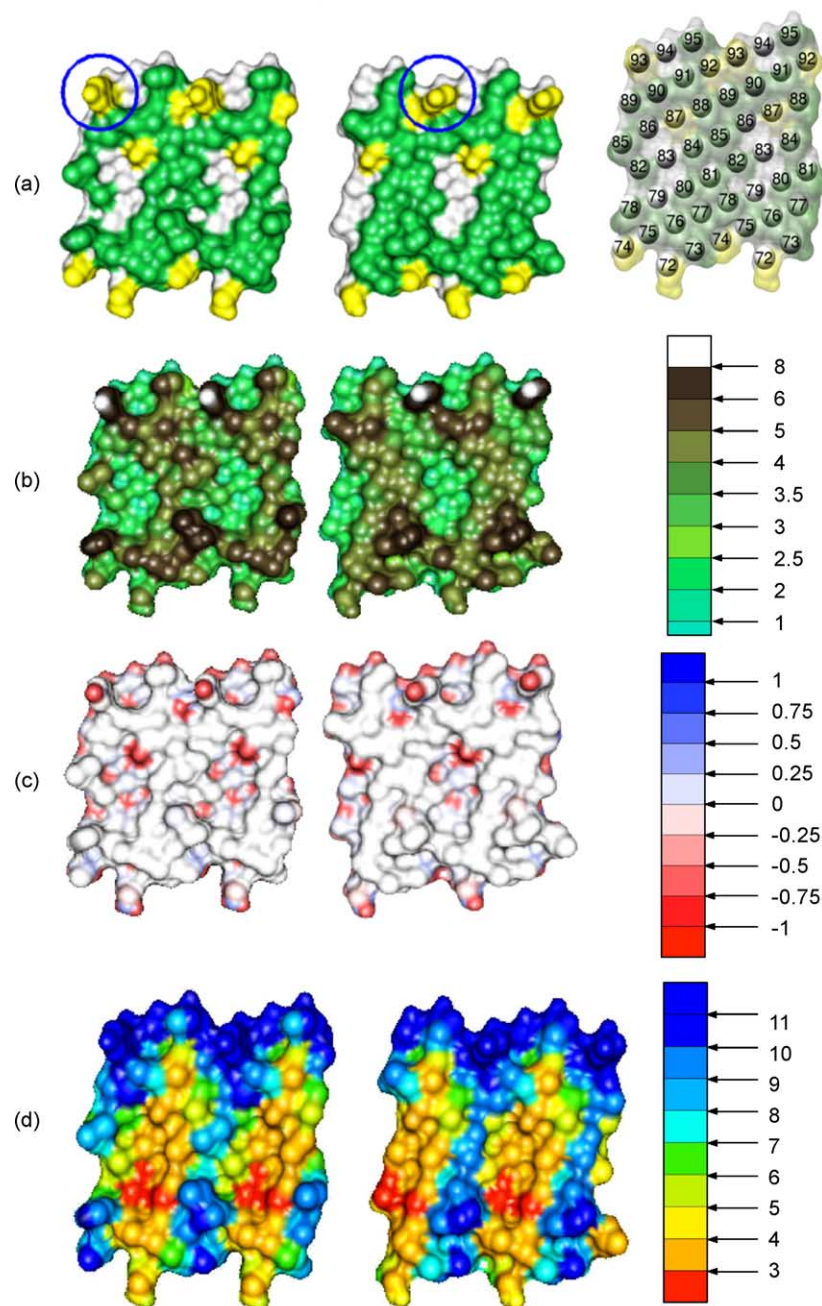


Fig. 5. Projection and coloring schemes. Illustration of several of the different coloring schemes to aid interpretation of helical surfaces. The transmembrane helix of glycoprotein A (1AFO), the segment from residue 72 to 95 “EITLIIFGVMAGVIGTILLISYGI” (the first residues are found at the bottom of the projection), has been colored according to four different codes. (a) Residue type (Hydrophobic scheme). (b) Distance from helix axis (Topology scheme) ranging from 1 to over 8 Å. (c) Atomic charge (Electrostatics scheme). (d) Distance from the other member of the homodimer (Pairwise scheme) in Å. At the right of panel (a) is shown a map, helical net, to aid in locating particular residues on the projection.

some kind of deformation on at least one of the interacting helices this may not be possible. This is confirmed by examining the complementary part of the interface on the interacting helix (helix 4), where we can see that this helix has a severe kink, resulting in a hole in the projection. We can also see that the upper (blue) interface runs in a slightly different direction along the helix surface than the lower (cyan) interface.

A second example of a simple interface is the red one on the lower right corner of Fig. 5b (helix 6), there we can see a big red patch in the middle of the projection and two smaller ones green (top) and purple (bottom). This clearly indicates that this helix interacts with three other partners. We can see groups of dark colored red atoms and light colored ones for instance near the bottom of the interface. On the corresponding red patch on the neighbor (helix 5) we can

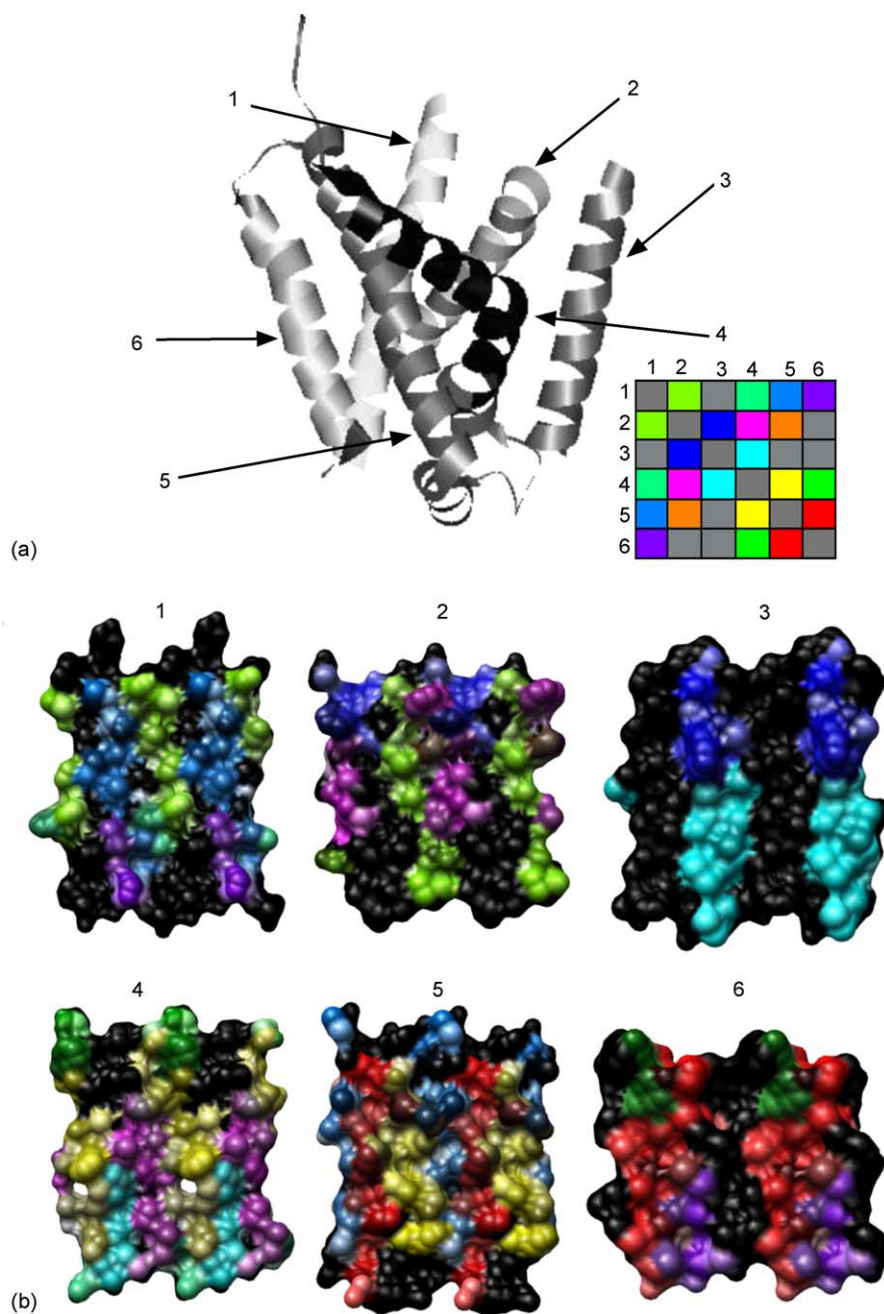


Fig. 6. Fumarate reductase Illustration of the utility of Ptuba in the analysis of helix-helix interactions in fumarate reductase (1L0V). (a) Overall organization of the helical bundle. Inset, interaction matrix describing the hue of each interface. (b) Helix projections colored according to the interface (multiple scheme). See text for details of the color scheme.

see a prominent group of dark red atoms in the middle and a group of light colored ones far below. Inferring distances from the previously described color codes we can say that the atoms near the bottom of the interface are in close interaction whereas some in the middle are farther apart or partially shared with other interfaces that are not in the outer helix's line of sight. The green patch is interaction with helix 4 and the purple patch on the bottom interacts with helix 1.

Helix 1 is different from helix 2 because it has two major interfaces side by side with helix 2 (yellow green) and helix

5 (blue), a small one with helix 6 (purple) and a very small one with helix 4 (blue green) between the two major interfaces. This indicates that the helix is more embedded in the bundle than helix 3 but is not part of the bundle core since we can still see black patches between the two major interfaces.

Most of the helices have at least four interfaces (helices 5, 4, 2 and 1) and comfortably embedded in the bundle. On helix 2 we see a black patch that becomes wider as we move to the lower portions of the helix. Thus, this helix interacts

mainly via its upper portion while the lower portion points to the exterior and is partially exposed. Interfaces in helix 2 have varied sizes that range from the big interface with helix 1 (green) to the minimalist interface with helix 5 (gold) that spans three atoms. The small interface with helix 3 (blue) is next to the medium sized interface with helix 4 (magenta) that is cut in half by the very small interface with helix 5 (gold). If the atoms in the small interface were shared between the last two interfaces, they would be gray. However, the atoms on the gold interface are darker but are not gray. Therefore they are not shared with the magenta interface. We see no such segmentation on the magenta patch on helix 4. This can be explained by the fact that interfaces can be supported by different portions of a helix even if they interact with the same portion of another helix. This is especially true with the case of kinked helices such as helix 4.

Helix 5 is similar to helix 4 in the sense that its interfaces span most of the surface of the projection. Here, three major interfaces with helix 4 (yellow), with helix 1 (blue) and with helix 6 (red) side by side cover most of the surface. This means that this helix forms with helix 4 the core of the

bundle. We can also see the gold in the middle of the projection just beneath two prominent dark blue atoms. It seems likely that in a 3D structure we would have missed this interaction. Thanks to Ptuba and the corresponding surface patch on helix 2 we have not. This is specially interesting for an interaction like this one (between an Arg and a His) because, given the environment, this kind of interaction tends to be particularly strong. Among other small features we can notice that some atoms are shared among the interfaces. They are colored gray, as can be seen in the middle of the projection between the yellow and blue interfaces.

Finally, helix 4 is a deeply embedded helix like helix 5 as indicated by the absence of black among the surface colors. We can tell this is a severely kinked helix thanks to the hole in the middle of the projection. This hole appears because kinks change the density distribution of the side chains making it lower on the outer side of the kink. We can also see the advantage of duplicating the projection in order to go beyond  $360^\circ$  as without it we could have missed the hole that is found between the merged projections. This helix interacts mainly with helix 5 (yellow), helix 2 (magenta) and helix 3

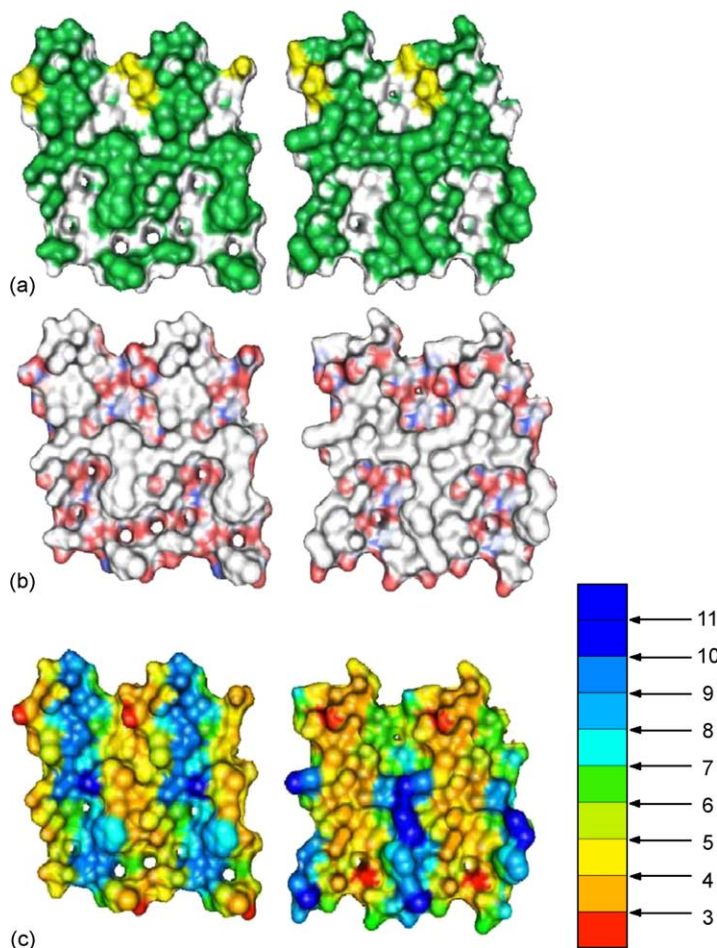


Fig. 7. Projections of the Erb-B2 transmembrane helix structure extracted from a molecular dynamics calculation. The sequence contains an oncogenic mutation. They are colored according to the hydrophobic scheme (a), the electrostatics scheme (b) and the Pairwise scheme (c) that represents the distance between the dimers in Å.

(cyan), but also has a small interaction with helix 6 (green top) and a very small one with helix 1 (blue green at the bottom). There are gray patches where several interfaces “merge”, e.g. the area just beneath the hole in the middle of the projection and above the cyan and blue green interface. This indicates not only those atoms or residues have an ability to interact with multiple partners but also their importance in the bundle structure acting as a cohesive joint allowing this specific kind of helical infrastructure to exist.

### 5.3. ErbB2 transmembrane helices

Analyzing multiple structures and grasping the variations among them is not an easy task. Molecular dynamics is a technique that generates multiple conformations over time and we think Ptuba can be useful for the visual analysis of such data sets. Our model here consists of two helices, from a homodimer of the transmembrane region of ErbB2. The ErbB2 dimer plays an important role in tyrosine kinase activation and its mutated forms have been linked to oncogenesis.

In Fig. 7, we show projections of the transmembrane helix of a mutated ErbB2. These structures are instantaneous conformations of the two monomers extracted from a molecular dynamics simulations [37]. The hydrophobicity scheme (Hydrophobic) indicates an important glutamate in the form of a yellow patch. The holes seen in the lower part of the left hand monomer on Fig. 7a are the result of a dynamic deformation (a widening) at the end of the helix. We can see that whereas the middle portion is well conserved, the upper portion suffers small changes from one monomer to the other, visible in particular as changes in the shape of the white patch with this coloring scheme. The lower portion changes more significantly modifying not only the side chains conformation but also the helicity of this portion of the helix, visible as the appearance and disappearance of holes in the projection, modifications in the shapes of white/green patches and changes in relief. In Fig. 7b, using the electrostatics scheme (Electrostatics) we can easily appreciate how the structural differences dramatically modify the surface charge distribution. The main features here would be the glutamate and the exposed backbone on the upper portion and the exposed backbone on the lower portion (plus the deformation derived exposure on the left hand monomer). Since this simulation is performed in vacuo we could suggest that the parts where the greatest charges are exposed in the surface will most likely participate in the helix interactions. Finally, in Fig. 7c the interface (Pairwise) between each monomer and its partner confirms that the glutamate is involved in a strong interaction as we can appreciate from the position and color of the atoms in the residue (in the middle, in red). We can also see that a small cluster of exposed charges on the right hand monomer interacts with the terminus of the other monomer. In fact, although exposing more charges, the deformation by its dynamical nature does not establish a

lasting interaction with the exposed backbone on the other homodimer.

The different color patches shown in the various panels of Fig. 7 also illustrate the plasticity associated to the structure of transmembrane domains, as seen by comparing the individual helices in the dimeric structure. These changes are allowed by conformational transitions that involve both side chain and backbone and alter the potential association surfaces. The appreciation of such rearrangements which is a difficult task in a 3D context is made easier by the Ptuba projection surface. Thus, Ptuba could be a valuable tool in the analysis of molecular dynamics simulations of membrane proteins.

## 6. Conclusion

We believe this visualization method will be useful for the study of interactions between helices as it helps in extracting useful information from 3D structures. As we have seen, this method allows us to go beyond the structural deformations in the helices and gain insight into their interactions with another helix or multiple helical partner in a more accessible way. This is achieved thanks to adapted coloring schemes and the fact that the analysis takes place outside a 3D space that usually brings difficulties to comprehension and visualization. Finally, with the increasing number of membrane protein structures, we believe that new tools to extract useful information out of this experimental data sets will become increasingly necessary.

## Acknowledgments

We would like to thank Richard Lavery for the source code of pCurves. This work has been supported by the CNRS (Centre National de La Recherche Scientifique) program PGP (Protéomique et Génie des Protéines). J.A.L. is also supported by a grant from the French Education Ministry

## References

- [1] J.L. Popot, D.M. Engelman, Membrane protein folding and oligomerization: the two-stage model, *Biochemistry* 29 (1990) 4031–4037.
- [2] D.M. Engelman, Y. Chen, C.N. Chin, A.R. Curran, A.M. Dixon, A.D. Dupuy, A.S. Lee, U. Lehnert, E.E. Matthews, Y.K. Reshetnyak, A. Senes, J.L. Popot, Membrane protein folding: beyond the two stage model, *FEBS Lett.* 555 (2003) 122–125.
- [3] W.P. Russ, D.M. Engelman, The GxxxG motif: a framework for transmembrane helix-helix association, *J. Mol. Biol.* 296 (2000) 911–919.
- [4] K.G. Fleming, D.M. Engelman, Specificity in transmembrane helix-helix interactions can define a hierarchy of stability for sequence variants, *Proc. Natl. Acad. Sci. U.S.A.* 98 (2001) 14340–14344.
- [5] A.W. Partridge, A.G. Therien, C.M. Deber, Polar mutations in membrane proteins as a biophysical basis for disease, *Biopolymers* 66 (2002) 350–358.

- [6] S. Sukharev, M. Betanzos, C.S. Chiang, H.R. Guy, The gating mechanism of the large mechanosensitive channel MscL, *Nature* 409 (2001) 720–724.
- [7] H. Valadie, J.J. Lacapre, Y.H. Sanejouand, C. Etchebest, Dynamical properties of the MscL of *Escherichia coli*: a normal mode analysis, *J. Mol. Biol.* 332 (2003) 657–674.
- [8] C. Toyoshima, H. Nomura, Y. Sugita, Structural basis of ion pumping by Ca(2+)-ATPase of sarcoplasmic reticulum, *FEBS Lett.* 555 (2003) 106–110.
- [9] C. Toyoshima, H. Nomura, Structural changes in the calcium pump accompanying the dissociation of calcium, *Nature* 418 (2002) 605–611.
- [10] G.N. Ramachandran, V. Sasisekharan, Conformation of polypeptides and proteins, *Adv. Protein Chem.* 23 (1968) 283–437.
- [11] G.N. Ramachandran, C. Ramakrishnan, V. Sasisekharan, Stereochemistry of polypeptide chain configurations, *J. Mol. Biol.* 7 (1963) 95–99.
- [12] C. Ramakrishnan, G.N. Ramachandran, Stereochemical criteria for polypeptide and protein chain conformations II. Allowed conformations for a pair of peptide units., *Biophys. J.* 5 (1965) 909–933.
- [13] B.R. Thomas, Sequence diagrams and the presentation of structural and evolutionary relationships among proteins, *Biochimie* 57 (1975) 271–276.
- [14] L. Lemesle-Varloot, B. Henrissat, C. Gaboriaud, V. Bissery, A. Morgat, J.P. Mornon, Hydrophobic cluster analysis: procedures to derive structural and functional information from 2-D-representation of protein sequences, *Biochimie* 72 (1990) 555–574.
- [15] R.R. Gabdouliline, R.C. Wade, D. Walther, MolSurfer: a macromolecular interface navigator, *Nucleic Acids Res.* 13 (2003) 3349–3351.
- [16] A.D. McLachlan, Coiled coil formation and sequence regularities in the helical regions of alpha-keratin, *J. Mol. Biol.* 124 (1978) 297–304.
- [17] P.C. Kahn, Defining the axis of a helix, *Computers Chem.* 13 (1989) 185–189.
- [18] J. Åqvist, A simple way to calculate the axis of an  $\alpha$  helix, *Comput. Chem.* 10 (1986) 97–99.
- [19] J.A. Christopher, R. Swanson, T.O. Baldwin, Algorithms for finding the axis of a helix: fast rotational and parametric least-squares methods, *Comput. Chem.* 3 (1996) 339–345.
- [20] L. Pauling, R.B. Corey, H.R. Branson, The structure of proteins; two hydrogen-bonded helical configurations of the polypeptide chain, *Proc. Natl. Acad. Sci. U.S.A.* 4 (1951) 205–211.
- [21] F.H.C. Crick, The packing of alpha-helices: simple coiled-coils, *Acta Crystallogr.* 6 (1953) 689–697.
- [22] D. Walther, F. Eisenhaber, P. Argos, Principles of helix-helix packing in proteins: the helical lattice superposition model, *J. Mol. Biol.* 255 (1996) 536–553.
- [23] S. Jayasinghe, K. Hristova, S.H. White, MPTopo: a database of membrane protein topology, *Protein Sci.* 10 (2001) 455–458.
- [24] F.S. Cordes, J.N. Bright, M.S. Sansom, Proline-induced distortions of transmembrane helices, *J. Mol. Biol.* 323 (2002) 951–960.
- [25] R.P. Riek, I. Rigoutsos, J. Novotny, R.M. Graham, Non-alpha-helical elements modulate polytopic membrane protein architecture, *J. Mol. Biol.* 306 (2001) 349–362.
- [26] E. Strandberg, S. Morein, D.T. Rijkers, R.M. Liskamp, P.C. van der Wel, J.A. Killian, Lipid dependence of membrane anchoring properties and snorkeling behavior of aromatic and charged residues in transmembrane peptides, *Biochemistry* 41 (2002) 7190–7198.
- [27] E. Dimas, D. Briassoulis, 3D geometric modelling based on NURBS: a review, *Adv. Eng. Software* 30 (1999) 741–751.
- [28] H. Sugeta, T. Miyazawa, General method for calculating helical parameters of polymer chains from bond lengths, bond angles and internal-rotation angles, *Biopolymers* 5 (1967) 673–679.
- [29] D.A. Pearlman, D.A. Case, J.W. Caldwell, W.R. Ross, T.E. Cheatham III, S. DeBolt, D. Ferguson, G. Seibel, P. Kollman, AMBER, a computer program for applying molecular mechanics, normal mode analysis, molecular dynamics and free energy calculations to elucidate the structures and energies of molecules, *Comp. Phys. Commun.* 91 (1995) 1–41.
- [30] J. Nathans, T. Piantanida, R. Eddy, T. Shows, D. Hogness, Molecular genetics of inherited variation in human color vision, *Science* 232 (1986) 203–210.
- [31] J. Neitz, G. Jacobs, Polymorphism of the long-wavelength cone in normal human color vision, *Nature* 323 (1986) 623–625.
- [32] J. Neitz, G. Jacobs, Polymorphism in normal human color vision and its mechanism, *Vis. Res.* 30 (1990) 620–636.
- [33] J. Neitz, M. Neitz, G. Jacobs, More than three cone pigments among people with normal color vision, *Vis. Res.* 33 (1993) 117–122.
- [34] C.C. Huang, G.S. Couch, E.F. Pettersen, T.E. Ferrin, Chimera: an extensible molecular modeling application constructed using standard components, *Pacific Symposium on Bio Computing* 1 (1996) 724.
- [35] H. Sklenar, C. Etchebest, R. Lavery, Describing protein structure: a general algorithm yielding complete helicoidal parameters and a unique overall axis, *Proteins* 6 (1989) 46–60.
- [36] K.R. Mackenzie, D.M. Engelman, Structure-based prediction of the stability of transmembrane helix-helix interactions: the sequence dependence of glycophorin A dimerization, *Proc. Natl. Acad. Sci. U.S.A.* 95 (1998) 3583–3590.
- [37] J.P. Duneau, N.N. Garnier, M. Genest, Insight into signal transduction: structural alterations in transmembrane helices probed by multi-1 ns molecular dynamics simulations, *J. Biomol. Struct. Dyn.* 15 (1997) 555–572.